Supplementary Data

Development of Targeted Nanoparticles Loaded with Antiviral Drugs for SARS-CoV-2 Inhibition

Vanna Sanna,[a,1] Sandro Satta,[b,1] Tzung Hsiai,[b] and Mario Sechi[c,] *

[a]*Nanomater S.r.l., Alghero 07041, Italy;* [b]*Department of Medicine, David Geffen School of Medicine, University of California, Los Angeles, California 90095, United States;* [c]*Department of Medical, Surgical, and Experimental Sciences, Laboratory of Drug Design and Nanomedicine, University of Sassari, Sassari 07100, Italy*

Contents

Figure S1A. Structures of "alkylated ligands" as model/surrogate of the *tri*-block-PEGylated copolymers used for docking calculations: PEG-ACL (orange), PEG-DCL (green), PEG-CPL (blue), and PEG-TAPI-2 (magenta). The site and mode of conjugation, with the short chain to simulate the polymer (grey) are indicated.

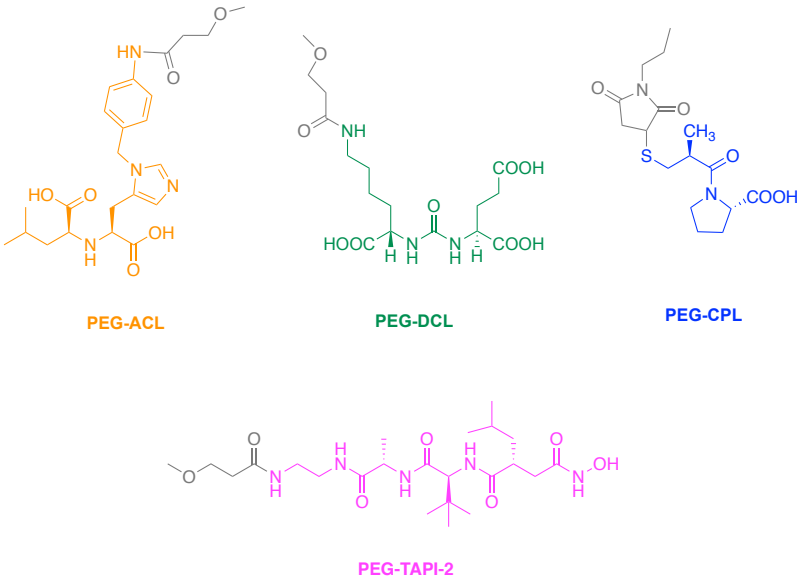

Figure S1B. 3D interaction images of the ligand **4 (A**, magenta**)** and its PEGylated model **(B)**, in the TACE active site. Zinc ion cofactor is represented as red sphere.

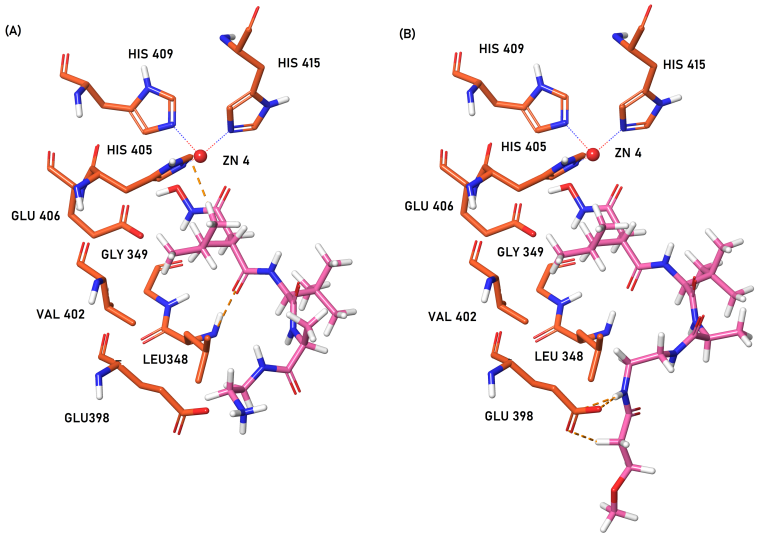

Scheme S1. Synthesis of copolymer PLGA-PEG-NHS.[a]

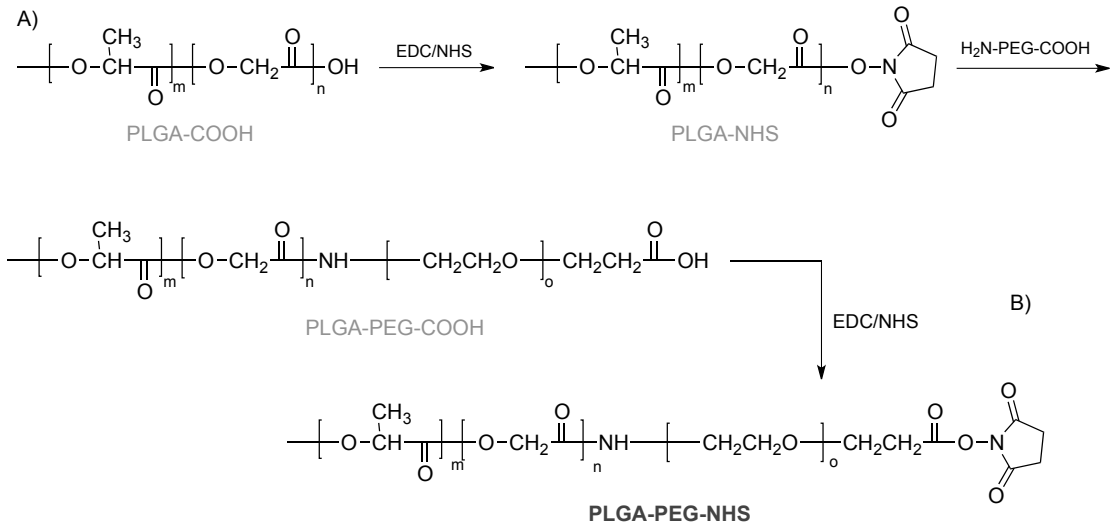

[a]**Reagents and conditions:** A) *i)* NHS, CH_2Cl_2, EDC•HCl, N_2, room temperature for 12 h, N_2; (*ii*) $CHCl_3$, DIPEA, r.t. for 24 h, N_2. B) NHS, CH_2Cl_2, EDC•HCl, N_2, r.t. for 12 h, N_2.

A) Synthesis of PLGA-PEG-COOH di-Block-Copolymer [1-3]. Briefly, to a solution of PLGA-COOH (4.0 g, 0.221 mmol) in anhydrous CH_2Cl_2 (15 mL), *N*-hydroxysuccinimide (NHS, 0.102 g, 0.884 mmol., ~4 equiv) and 1-ethyl-3-(3-dimethylaminopropyl)carbodiimide hydrochloride (EDC•HCl, 0.182 g, 0.950 mmol, ~4.3 equiv.) were added, and the reaction mixture was magnetically stirred at room temperature for 12 h under nitrogen atmosphere. PLGA–NHS was obtained by precipitation with cold diethyl ether (Et_2O, 15 mL) as a white solid, which was filtered, and repeatedly washed in a cold mixture of Et_2O and (few drops of) MeOH, then treated with nitrogen and dried under vacuum to remove solvent (~95% yield). The intermediate PLGA–NHS (3.5 g, 0.200 mmol) was dissolved in anhydrous $CHCl_3$ (12 mL), NH_2–PEG–COOH (0.91 g, 0.26 mmol; 1.3 equiv) and *N,N*-diisopropylethylamine (DIPEA) (0.14 mL, 0.80 mmol; 4 equiv) were added, and the reaction reaction was magnetically stirred at room temperature for 24 h under nitrogen atmosphere. The mixture was then repeatedly treated with cold Et_2O to remove unreacted PEG, to afford the PLGA–PEG block copolymer (~95% yield), which was dried under vacuum, characterized, and used for NP preparation without any further purification. ^{1}H-NMR (400 MHz, $CDCl_3$) δ 5.23 (m, OC-C*H*(CH_3)O, PLGA), 4.78 (m, OC-CH_2O, PLGA), 3.65 (s, CH_2CH_2O, PEG), 1.56 (brs, OC-CHCH_3O, PLGA) [1-3].

B) Synthesis of PLGA-PEG-NHS di-Block-Copolymer [1-3]. To a solution of PLGA-PEG-COOH (2.5 g, 0.1225 mmol) in anhydrous CH_2Cl_2 (9 mL), NHS (56 mg, 0.490 mmol, ~4 equiv) and EDC•HCl (101 mg, 0.5267 mmol, ~4.3 equiv) were added, and the solution was magnetically stirred at room temperature for 12 h under nitrogen atmosphere. The activated PLGA-PEG-NHS copolymer was obtained by precipitation with cold diethyl ether (Et_2O, 10 mL) as a white solid (~92% yield), following the procedure previously used to obtain the PLGA- NHS intermediate.

Scheme S2. Synthesis of copolymer PLGA-PEG-mal.[a]

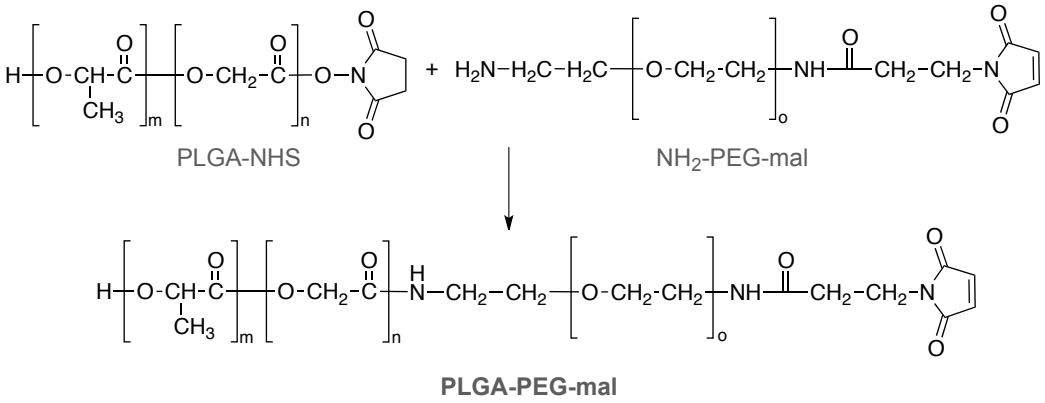

[a]**Reagents and conditions:** (*i*) $CHCl_3$, DIPEA, N_2, r.t. for 24 h.

Synthesis of PLGA-PEG-mal [4]. To a solution of PLGA-NHS (1.0 g, 0.057 mmol) in anhydrous $CHCl_3$ (7 mL), NH_2-PEG-maleimide (0.80 g, 0.228 mmol, 4 equiv.) in anhydrous $CHCl_3$ (5 mL) and was added DIPEA (0.1 mL, 0.57 mmol, 10 equiv.), and the solution was magnetically stirred at room temperature for 24 h under nitrogen atmosphere. The PLGA-PEG-mal copolymer was obtained by precipitation with cold Et_2O, then dried under vacuum, and used for NP preparation without further treatment (yield, 95%). ^{1}H-NMR (400 MHz, $CDCl_3$): δ 5.32-5.10 (m, 1H, -OC-C*H*(CH_3)O-, PLGA), 4.93-4.63 (m, 2H, -OC-C*H*$_2$O- PLGA), 3.64 (brs , 2H, -C*H*$_2$C*H*$_2$O-, PEG), 1.58 (brs , 3H, -OC-CH(C*H*$_3$)O-, PLGA) [4].

Figure S2. Characterization of PLGA-PEG-**1**: ^{1}H-NMR with pattern signals of PLGA-PEG fragment, and magnification of representative ACL (**1**) peaks (dotted window).

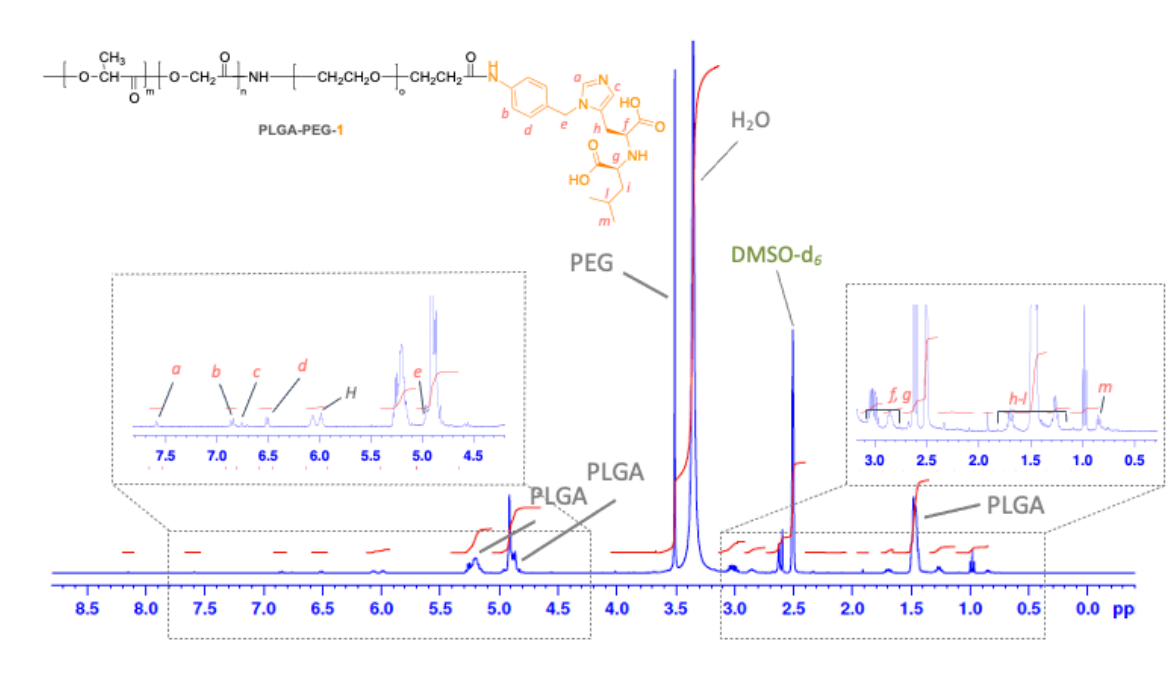

Figure S3. Characterization of PLGA-PEG-**2**: ^{1}H-NMR with pattern signals of PLGA-PEG fragment, and magnification of representative DCL (**2**) peaks (dotted window).

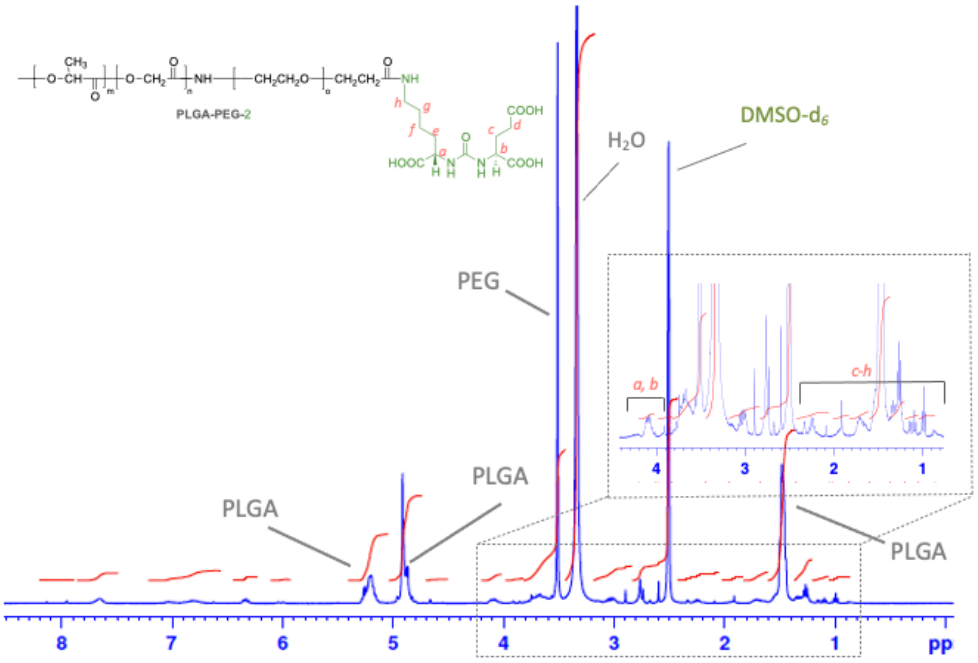

Figure S4. Characterization of PLGA-PEG-**3**: ^{1}H-NMR with pattern signals of PLGA-PEG fragment, and magnification of representative CPL (**3**) peaks (dotted window).

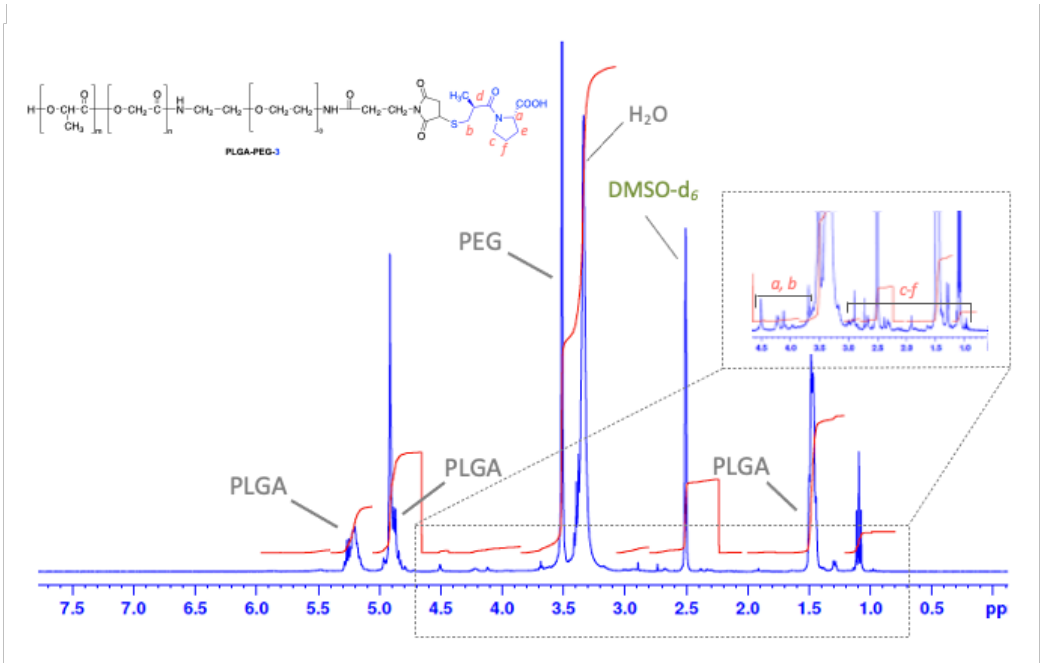

Figure S5. Characterization of PLGA-PEG-**4**: ^{1}H-NMR with pattern signals of PLGA-PEG fragment, and magnification of representative TAPI-2 (**4**) peaks (dotted window).

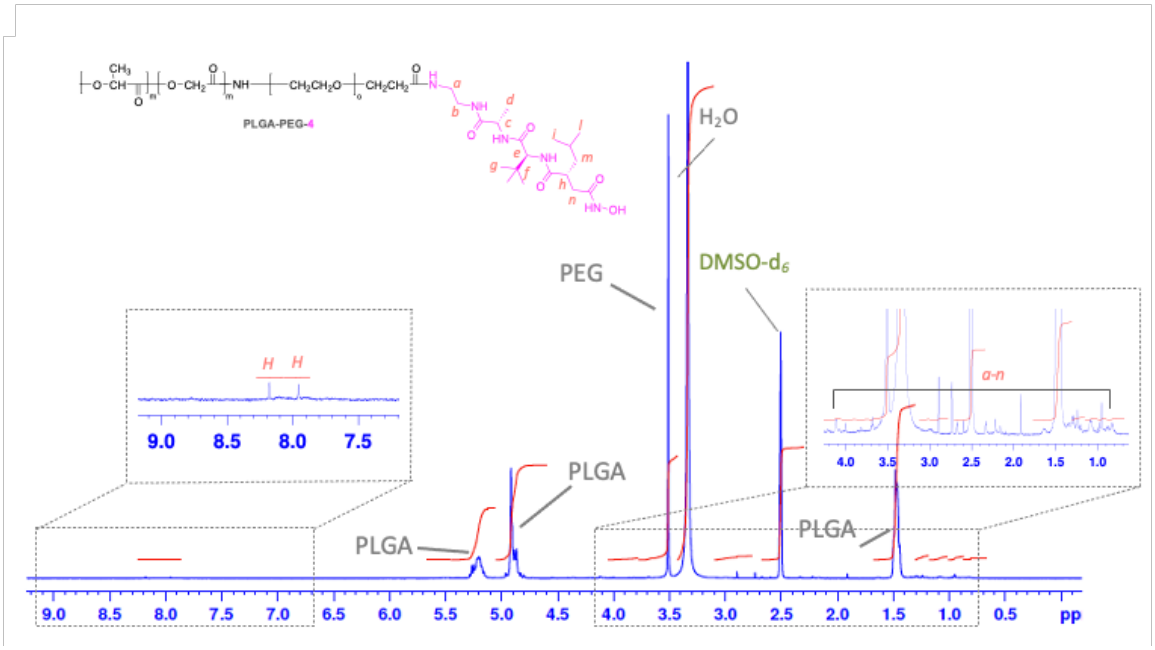

Figure S6. ^{1}H-NMR spectra of **1** recorded in DMSO-d_6 (**a**), DMSO-d_6 + D_2O **(b)**, and D_2O **(c)**.

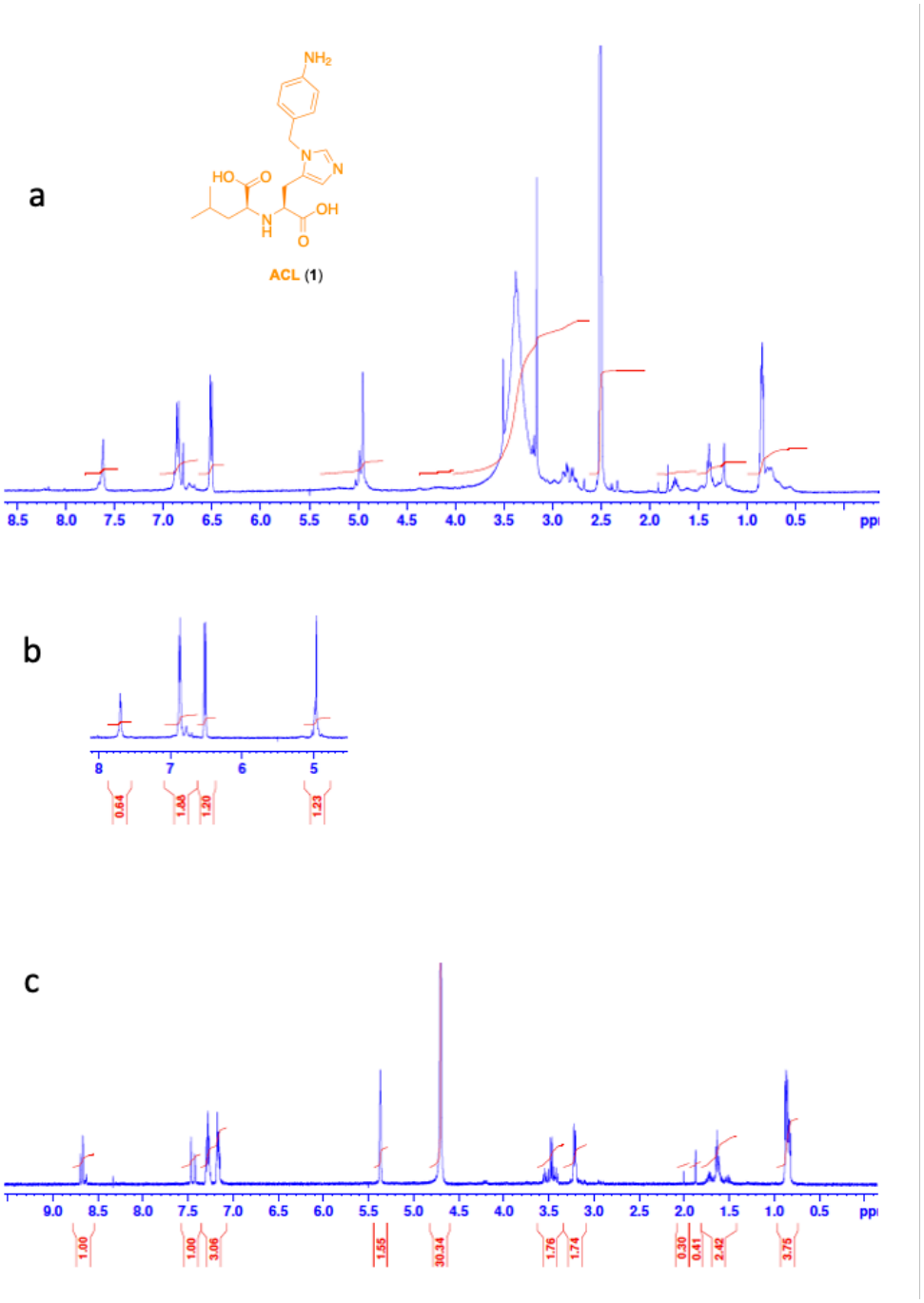

Figure S7. Top: 2D-NOESY spectrum of **1** recorded in D_2O **(a)**, with significative crosspeak indicating a NOE correlation for **1** conformer in *S,S* configuration **(b)**.

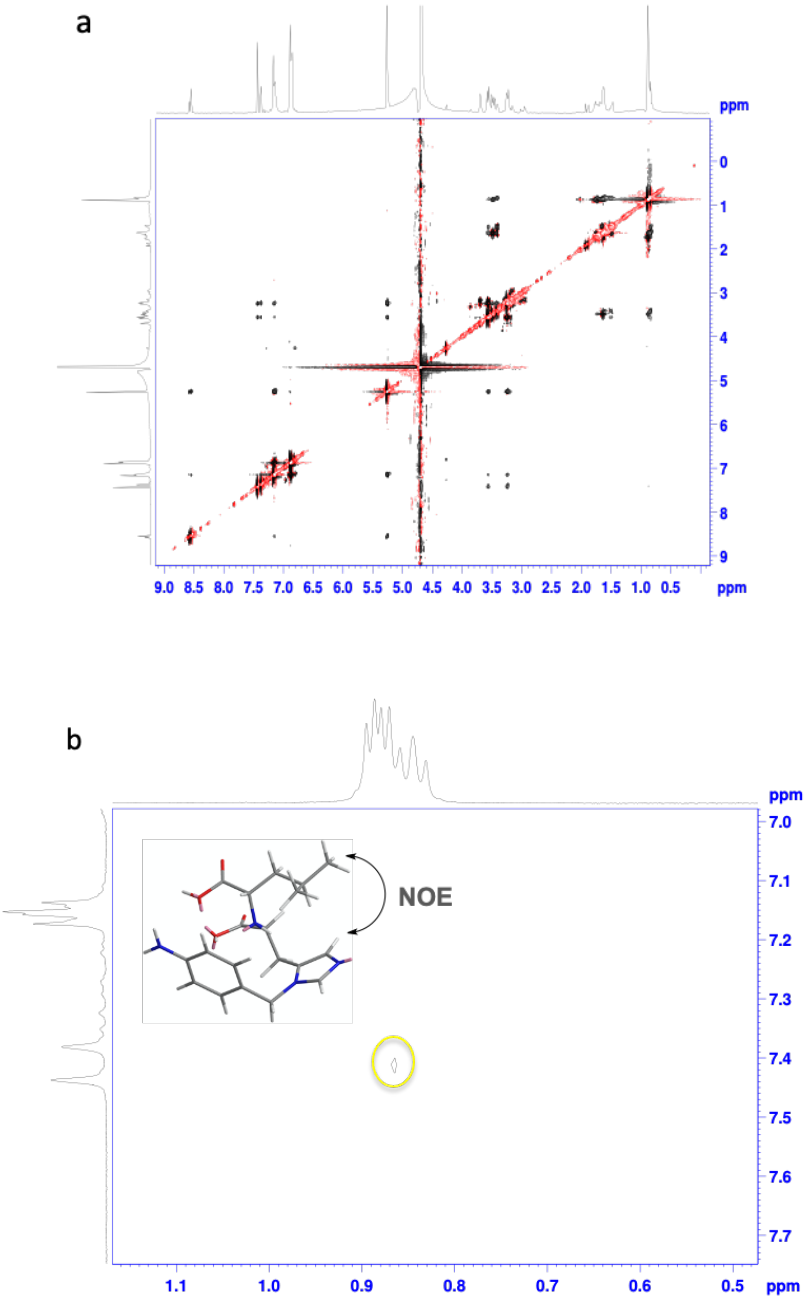

Figure S8. ^{13}C-NMR **(a)**, COSY **(b)** and HSQC **(c)** spectra of **1** recorded in DMSO.

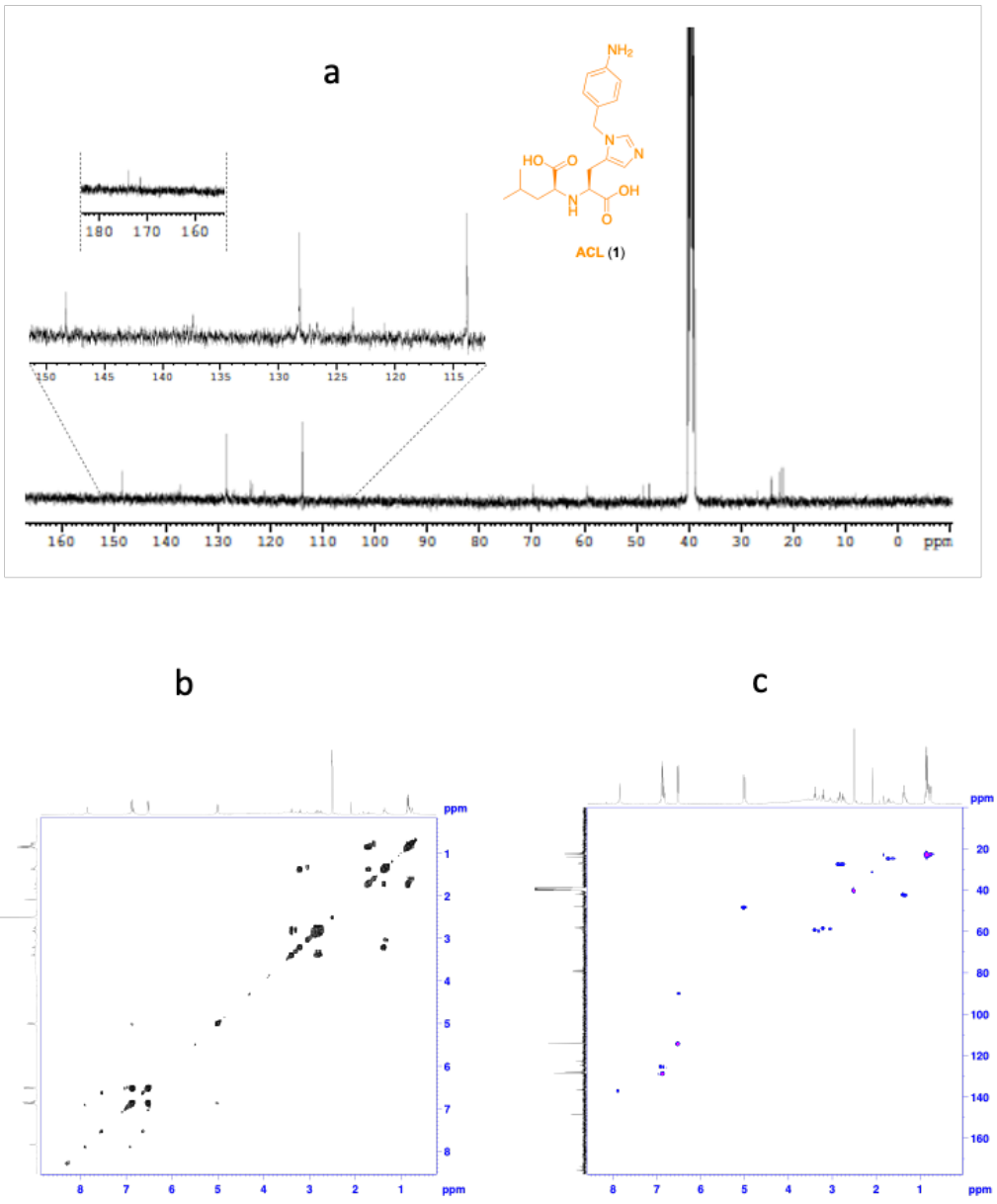

Figure S9. HRMS (ESI) spectra **(a, b)** of **1** calculated for $[C_{19}H_{26}N_4O_4+H]^+$ and $[C_{19}H_{26}N_4O_4+Na]^+$.

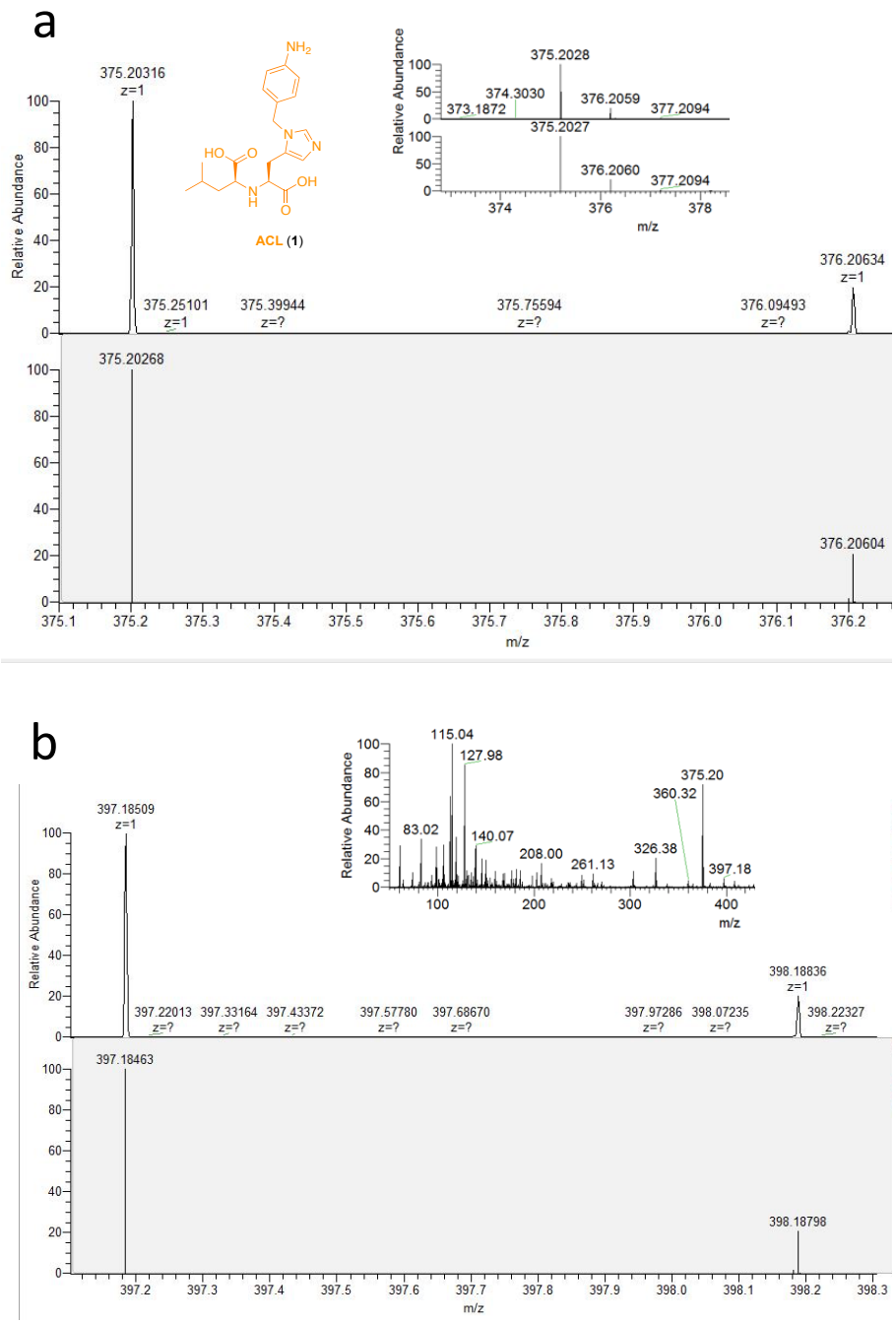

Figure S10. HPLC chromatogram of **1**.

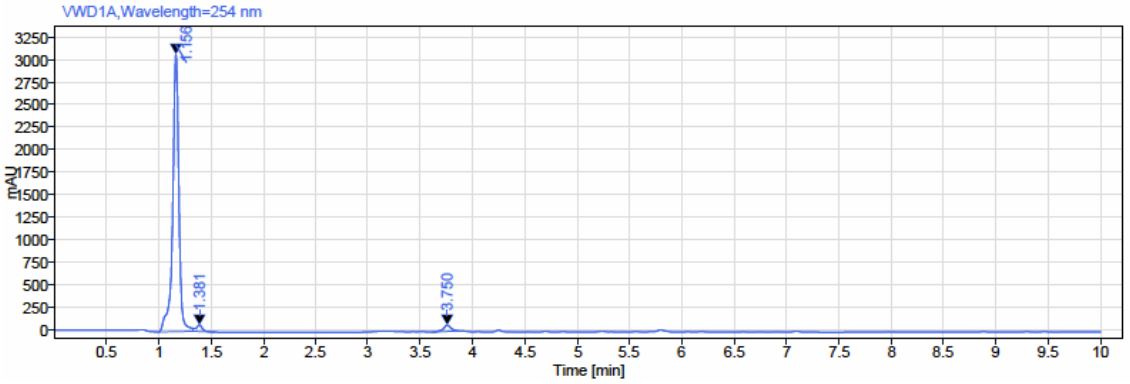

Signal: VWD1A,Wavelength=254 nm

RT [min]	Type	Width [min]	Area	Height	Area%	Name
1.156	BM m	0.06	12718.58	3084.24	95.11	
1.381	MM m	0.06	304.63	71.92	2.28	
3.750	BM m	0.07	349.58	68.76	2.61	
		Sum	13372.78			

Scheme S3. Synthesis of the synthon **11**.[a]

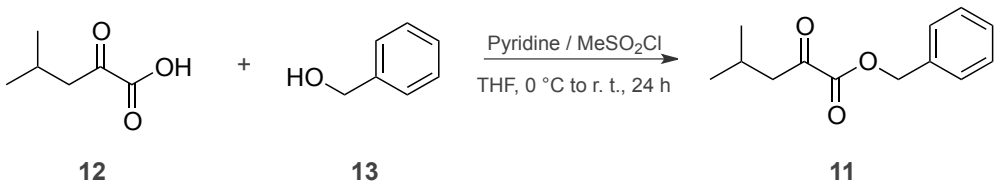

12 **13** **11**

Synthesis of benzyl 4-methyl-2-oxopentanoate (11) [6]**.** Benzyl α-ketoester **11** was synthesized by dissolving the commercially available benzyl 4-methyl-2-oxopentanoate (**12**) (5.0 g., 4.74 mL, 38.42 mmol, 1 equiv), benzyl alchool (**13**) (8.31 g., 7.95 mL, 76.84 mmol, 2 equiv) and pyridine (7.60 g., 7.67 mL, 96.05 mmol, 2.5 equiv), in THF (35 mL), cooled to 0 °C, under magnetic stirring, according to a previously reported method [5,6]. To this solution, mesyl chloride (5.28 g., 3.58 mL, 46.10 mmol, 1.2 equiv) was added dropwise, and the reaction mixture was then stirred at room temperature for 24 h. Next, the reaction was quenched with water (80 mL) and extracted with diehtyl ether (3 x 50 mL). The organic layers were dried over Na_2SO_4, filtered and concentrated in vacuo. The resulting crude product was purified by flash column chromatography on silica gel (petroleum ether / ethyl acetate = 95:5) to afford **11** as a colorless oil (97% yield). ^{1}H-NMR (400 MHz, $CDCl_3$) δ 7.39-7.36 (5H, m), 5.27 (2H, s), 2.71 (2H, d), 2.18 (1H, m), 0.95 (6H, d). MS (ESI), calculated for $C_{13}H_{16}O_3$ ($[M]^+$) 220 [6].

Scheme S4. Synthesis of **2**.

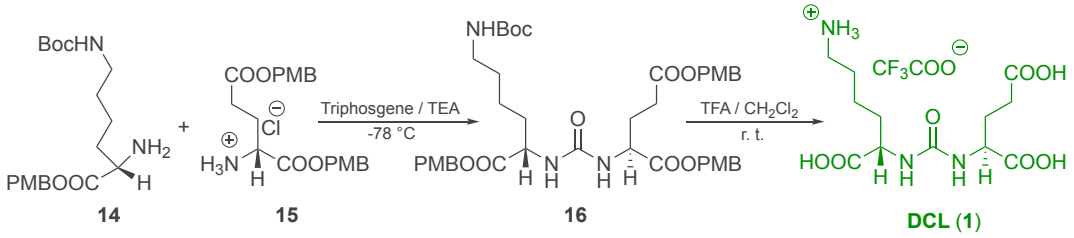

Preparation of 2-{[(5-amino-1-carboxypentyl)carbamoyl]amino}pentanedioic acid (2) [1-3]. The intermediate (10*S*,14*S*)-tris(4-methoxybenzyl)2,2-dimethyl-4,12-dioxo-3-oxa-5,11,13-triazahexadecane-10,14,16-tricarboxylate (**16**, 200 mg, 0.26 mmol) was dissolved in 5 mL 1:1 trifluoroacetic acid (TFA):CH_2Cl_2 solution and stirred at room temperature. After 3 h, the solution was evaporated, and the solid residue was triturated with dry Et_2O, filtered, and washed several times with dry Et_2O to yield **2** as a beige powder, which became amorphous after air exposure (yield: ~90%). ^{1}H-NMR (400 MHz, D_2O) δ 4.19− 4.12 (m, 2H), 2.93− 2.90 (m, 2H), 2.45− 2.41 (m, 2H), 2.14− 2.05 (m, 1H), 1.93− 1.76 (m, 2H), 1.67− 1.59 (m, 3H), 1.45−1.30 (m, 2H). ^{13}C-NMR (D_2O) δ 177.3, 177.1, 176.9, 176.4, 159.3, 66.0, 52.9, 52.6, 39.2, 30.4, 30.1, 26.2, 26.1, 22.0, 14.1. HRMS (ESI), calculated for $C_{12}H_{22}N_3O_7$ ($[M+H]^+$) 320.1450. Anal. ($C_{12}H_{21}N_3O_7$ • 1.15CF_3COOH • 0.65Et_2O) C, H, N [1-3,7].

Preparation of (10*S*,14*S*)-tris(4-methoxybenzyl)2,2-dimethyl-4,12-dioxo-3-oxa-5,11,13-triazahexadecane-10,14,16-tricarboxylate (16). The urea-based key intermediate **16** was synthesized by coupling of 2-amino-6-tert –butoxycarbonylaminohexanoic acid 4-methoxybenzyl ester (**14**) with bis-4-methoxybenzyl-L-glutamate hydrochloride (**15**) following the previously described procedures [1-3]. Briefly, triphosgene (0.50 g, 1.71 mmol) was placed onto a flame dried flask cooled to 0 °C, under nitrogen atmosphere, and a solution of **15** (1.89 g, 5.17 mmol, 3 equiv) and TEA (1.50 mL, 10.32 mmol, 6 equiv) dissolved in CH_2Cl_2 (10 mL) was added. The reaction mixture was stirred at 0 °C for 20 min. A mixture of **14** (2.90 g, 6.82 mmol, 3 equiv) and TEA (1.94 mL, 13.63 mmol, 6 equiv) in CH_2Cl_2 (7 mL) was then added, and the resulting mixture was allowed to warm to room temperature and stirred for 2 h. Product was extracted by CH_2Cl_2, washed with water and brine, and dried over Na_2SO_4. Purification by flash chromatography (80/20 CH_2Cl_2/EtOAc) afforded a yellow oil that solidified upon standing (yield: ~75%). ^{1}H-NMR (400 MHz, $CDCl_3$) δ: 7.26 (d, 6H), 6.87 (d, 6H), 5.52 (d, 2H), 5.13-4.98 (m, 6H), 4.76 (brs, 1H), 4.53-

4.48 (m, 1H), 4.50-4.43 (m, 1H), 3.79 (s, 9H), 3.04-2.96 (m, 2H), 2.40-2.34 (m, 2H), 2.14-2.11 (m, 2H), 1.94-1.70 (m, 2H), 1.60-1.56 (m, 2H), 1.42 (s, 9H), 1.25-1.22 (m, 2H). HRMS (ESI), calculated for $C_{41}H_{53}N_3O_{12}$ ($[M+H]^+$) 780 [1-3].

Figure S11. ^{1}H-NMR **(a)** and ^{13}C-NMR **(b)** spectra of **2** recorded in D_2O.

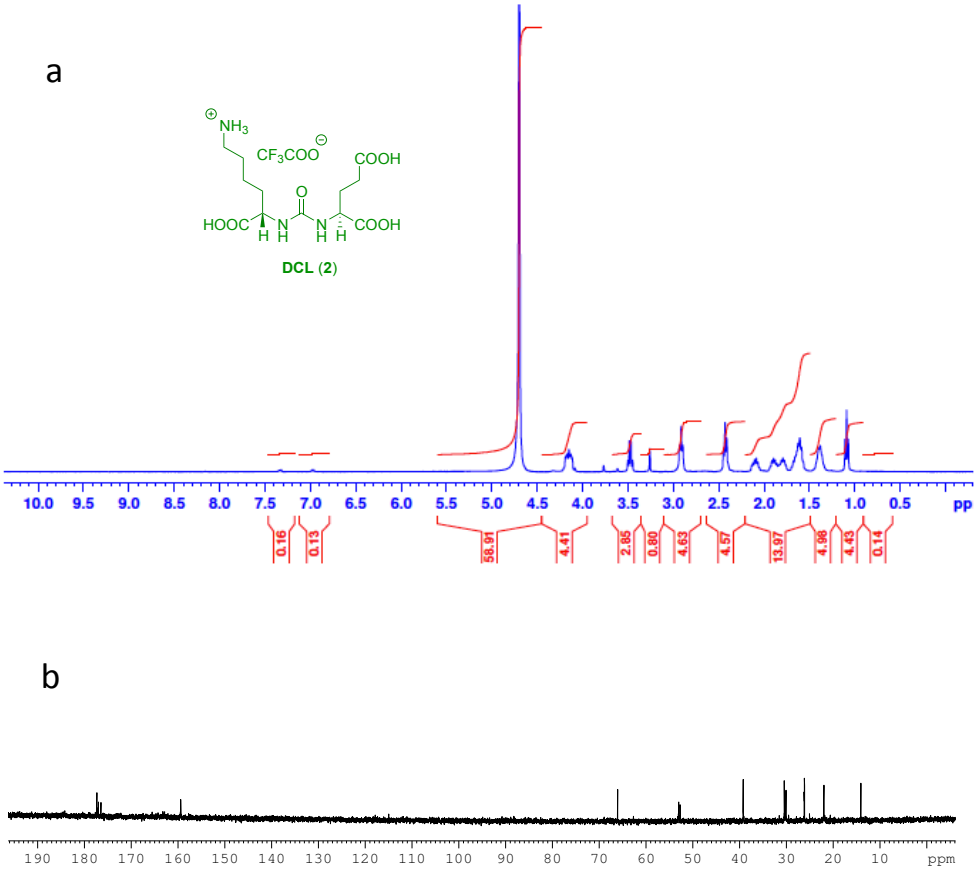

Figure S12. a, b) HRMS (ESI) of **2**, calculated for $C_{12}H_{22}N_3O_7$ ($[M+H]^+$).

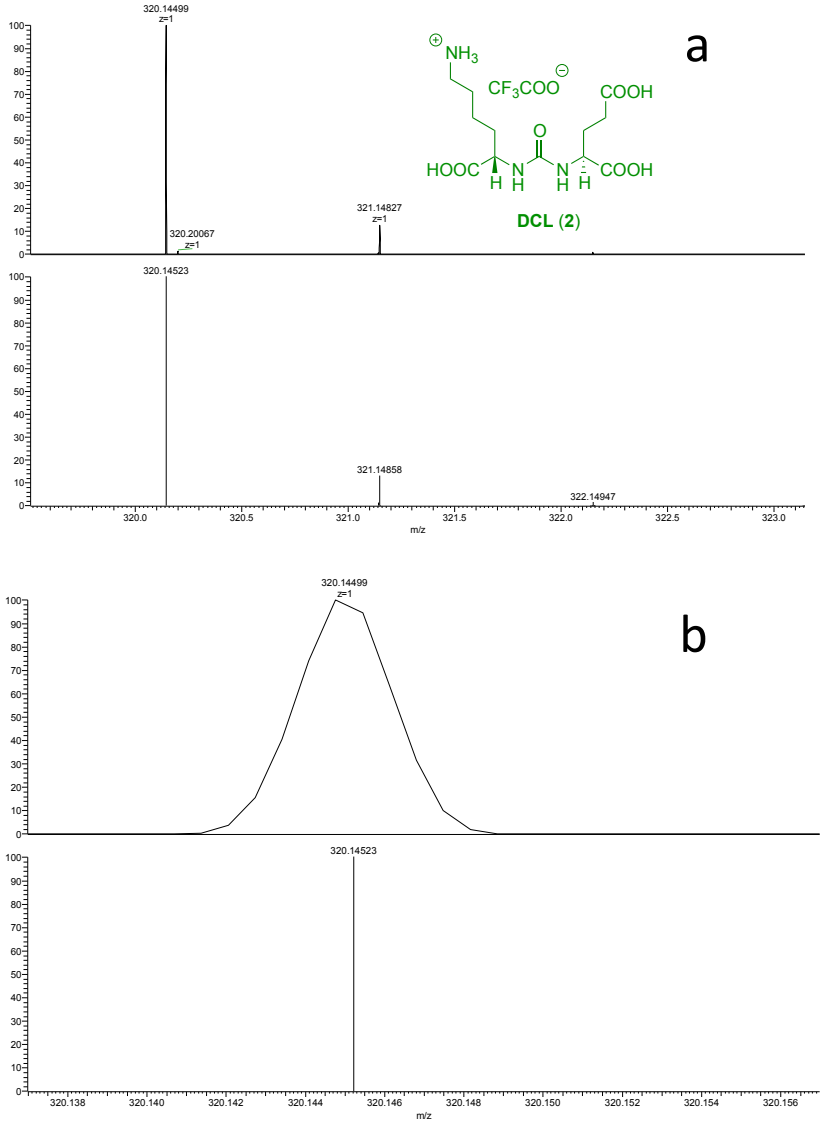

Figure S13. Microscopic images showing effect of TNP-**1**E and RDV on SARS-CoV-2 CPE induction. **(A)** Not infected VERO E6 cell monolayer as control (CTRL), and SARS-CoV-2 infected cells at 0.05_{MOI}, after 72 hours post infection. **(B)** SARS-CoV-2 infected VERO E6 after TNP-**1**E exposure at different concentrations. Unloaded NP were tested at the same NP w/v concentration (μg/mL) of the parent RDV-loaded nanosample (300, 60, 6 μg/mL, for TNP-**1**E, which correspond to 5, 1, 0.1 μM, for RDV-TNP-**1**, respectively). **(C)** SARS-CoV-2 infected VERO E6 after RDV exposure at different concentrations (5, 1, 0.1 μM) (scale bar 50 μm).

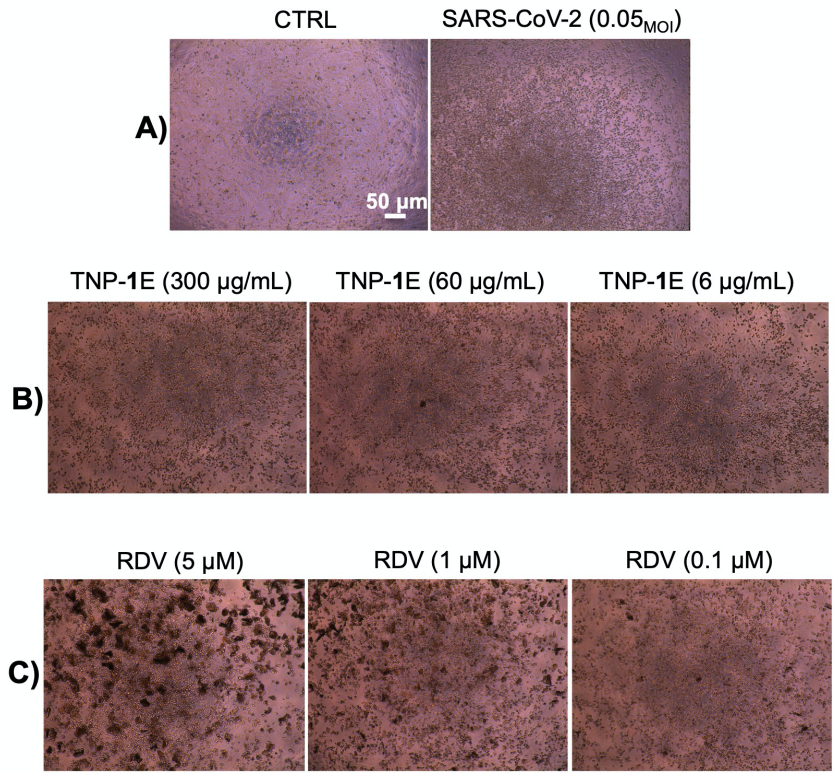

Figure S14. ACE2 exopeptidase activity by MLN-4760.

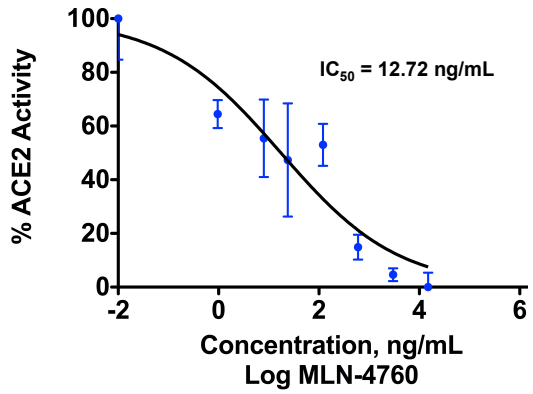

References

[1] V. Sanna, G. Pintus, A.M. Roggio, S. Punzoni, A.M. Posadino, A. Arca, S. Marceddu, P. Bandiera, S. Uzzau, M. Sechi, Targeted biocompatible nanoparticles for the delivery of (-)-epigallocatechin 3-gallate to prostate cancer cells, J. Med. Chem. 54 (2011) 1321–1332.

[2] V. Sanna, G. Pintus, P. Bandiera, R. Anedda, S. Punzoni, S. Sanna, V. Migaleddu, S. Uzzau, M. Sechi, Development of polymeric microbubbles targeted to prostate-specific membrane antigen as prototype of novel ultrasound contrast agents, Mol. Pharm. 8 (2011) 748-757.

[3] V. Sanna, C.K. Singh, R. Jashari, V.M. Adhami, J.C. Chamcheu, R. Islam, M. Sechi, H. Mukhtar, I.A. Siddiqui, Targeted nanoparticles encapsulating (-)-epigallocatechin-3-gallate for prostate cancer prevention and therapy, Sci. Rep. 7 (2017) 41573.

[4] V. Sanna, S. Nurra, N. Pala, S. Marceddu, D. Pathania, N. Neamati, M. Sechi, Targeted nanoparticles for the delivery of novel bioactive molecules to pancreatic cancer cells, J. Med. Chem. 59 (2016) 5209–5220.

[5] J.W. Yang, B. List, Catalytic Asymmetric Transfer Hydrogenation of α-Ketoesters with Hantzsch Esters, Org. Lett. 8 (2006) 5653–5655.

[6] W. Raimondi, O. Baslé, T. Constantieux, D. Bonne, J. Rodriguez, Activation of 1,2-Ketoesters with Takemoto's Catalyst toward Michael Addition to Nitroalkenes, Adv. Synth. Catal. 354 (2012) 563–568.

[7] Y. Chen, M. Pullambhatla, S.R. Banerjee, Y. Byun, M. Stathis, C. Rojas, B.S. Slusher, R.C. Mease, M.G. Pomper, Bioconjugate Chem. 23 (2012) 2377−2385.